SUPPLEMENTAL MATERIAL

Materials and Methods

Fecal Lipid Measurement

Mice were fed a high-fat/cholesterol diet (20% saturated fat, 0.15% cholesterol, Research Diet, Inc.) for 10 days. Then, feces were collected for 2 days and lipids were extracted. Total cholesterol, phospholipids, and triglycerides were determined.

Real-time PCR primer sequences

The following primers were used for mRNA measurement by Real-time PCR: 5'-ATTGGTCAAGCCAGCT-3' and 5'-TGTAGGCTCATCCACTAC-3' (mouse CD36), 5'-ATCCTCATCCTGGGCTTTGC-3' and 5'-GCAAGGTGATCAGGAGGTTGA-3' (mouse Npc1l1), 5'-AAAGTGAGGAGTGGACAGATGCT-3, and 5'-TGCCTGTGATCACGTCGAGTAG-3' (mouse Abcg8), 5'-GGTTTGGAGATGGTTATACAATAGTTGT-3' and 5'-TTCCCGGAAACGCAAGTC-3' (mouse Abca1), 5'-ACGGCCAGAAGCCAGAAGCCAGTAGTC-3' and 5'-GACCTTTTGTCTGAACTCCCTGTAG-3' (mouse Srb1), 5'-TCTGCTTCCGTTAAAGGTCACA-3' and 5'-CCTTTGCCCCCATCAAGAA-3' (mouse Mttp), and 5'-AGTCCCTTGCCCTTTGTACACA-3' and 5'-GATCCGAGGGCCTCACTAAAC-3' (18S RNA).

Electrophoretic Mobility Shift Assay

Electrophoretic mobility shift assays were performed with 32P-labeled fragments of the LPCAT3 promoter extending from nt -133 to - 97 in the presence of PPARα, RXR α, or both. WT and mutant oligonucleotide competitors were included at a 5-fold or 25-fold molar excess. Human PPARα and RXRα were translated in vitro using TNT T7 Quick Coupled Transcription/Translation System (Promega). Electrophoretic mobility shift reactions contained 10 mM HEPES (pH 7.5), 75 mM KCl, 1 mM EDTA, 0.05% (w/v)

Triton X-100, 10% glycerol, 1 mM DTT, 1 μg poly(dI-dC), 15–18 cpm probe, and 5 μL in vitro - translated PPARα and/or RXRα protein. After a 30-min incubation on ice, DNA-protein complexes were resolved on a 6% DNA retardation gel (Invitrogen) in 0.5x TBE. Gels were dried and subjected to autoradiography.

ChIP Assays

For mouse liver ChIP assays, frozen mouse liver from the fenofibrate study was crushed into powder. DNA-protein crosslinking was performed by mixing 50 mg liver powder with 0.5 mL of 1% formaldehyde in PBS containing 1 mM DTT and 1 mM PMSF and incubating 15 min at room temperature. Crosslinking was stopped by adding glycine to a final concentration of 0.125 M. Liver nuclei were isolated with a Dounce homogenizer in hypotonic solution followed by centrifugation at 4000 x g for 5 min. Mouse liver tissue ChIP assays were performed using a ChIP assay kit (Millipore, Billerica, MA) and anti-PPARα antibody (5 μg, Affinity BioReagents) or control rabbit IgG (Santa Cruz Biotechnology). DNA (1 μL) was subjected to PCR using mouse LPCAT3 promoter -1000 (forward primer: 5'-AAAGCCTACGTTCAATTTCCCAGTA-3') and mouse LPCAT3 promoter +55(reverse primer: 5'-AGAGCCTCTAGACCCACCCACCCGATTAT-3') for 35 cycles at an annealing temperature of 60°C.

SUPPLEMENTAL FIGURE LEGENDS

Supplemental Figure 1. LPCAT3 is the major LPCAT in small intestine and liver. (*A*) LPCAT3 mRNA in different mouse tissues measured by real-time PCR using total RNA. Adi, adipose tissue; Pan, pancreas; SI, small intestine; Spl, spleen; and Stom, stomach. (*B*) and (*C*) LPCAT1-4 mRNAs in the liver and small intestine of WT and LPCAT3 KO mice. Values are mean ± SD, n = 5. (*D*) Mendelian segregation of targeted LPCAT3 KO allele. Genomic DNA was extracted from the tail tip of 2-week-old mice for PCR analysis. WT mice have a 222-bp fragment, homozygous KO mice have a 326-bp fragment, and heterozygous mice have both.

Supplemental Figure 2. Western blots of LPCAT1, LPCAT2, and LPCAT4. (*A*) LPCAT1, 2, and 4 protein levels in enterocytes from WT and LPCAT3 KO enterocyte homogenates. (*B*) LPCAT1, 2, and 4 protein levels in liver from WT and LPCAT3 KO liver homogenates. Values are mean ± SD, n = 4.

Supplemental Figure 3. LPCAT3 deficient mice are smaller than WT mice. A representative litter of mice was monitored at 3, 5, 7, and 10 d after birth. Red arrows indicate homozygous KO mice. This is the representative of more than 30 litters. The KO mice were male and female. The average body weight (WT vs. KO) for day 3, day 5, day 7, and day 10 were: 2.5 ± 0.08g vs 1.4 ± 0.05g; 3.8 ± 0.25 vs 2.5 ± 0.12g; 5 ± 0.9 vs 3 ± 0.5g; and 7 ± 1.2 vs 3.5 ± 0.8g. Values are mean ± SD, n = 6.

Supplemental Figure 4. LPCAT3 deficient mice have normal liver morphology. Livers from LPCAT3 KO and WT mice were sectioned and stained with H&E. Representative images are shown (n = 5 animals of each type).

Supplemental Figure 5. ApoA-I protein and mRNA in enterocytes. (*A*) Western blots of apoA-I in WT and LPCAT3 KO enterocyte homogenates. (*B*) Quantification of apoA-I protein levels. (*C*) apoA-I mRNA levels in WT and LPCAT3 KO enterocytes. Values are mean ± SD, n = 4. *P<0.01.

Supplemental Figure 6. Phospholipid absorption in LPCAT3 KO mice. Male mice, at age 10-weeks-old, were gavaged with 0.1 µCi L-α-1-palmitory-2-arachidonyl-phosphatidylcholin [arachidonyl-1-^{14}C] in 15 µL olive oil. Blood was collected over 8 hr and measured for the presence of [^{14}C]-glycerolipids. Values are mean ± SE, n = 4. *P<0.05.

Supplemental Figure 7. LPCAT3 can be regulated by LXR and PPARs. (*A*) and (*B*), WT mice (C57BL/6) were treated with LXR agonist (T0901317, 35 mg/kg/d) or vehicle for 4 days. (*C*) and (*D*), WT mice (C57BL/6) were treated with PPARα agonist (Fenofibrate, 300 mg/kg/d) or vehicle for 4 days. Liver and small intestine LPCAT3 mRNA was measured by real-time PCR. Values are mean ± SD, n = 5, *P < 0.05, **P < 0.01.

Supplemental Figure 8. LPCAT3 promoter region contains functional PPAR-responsive elements (PPREs). (*A*) Four candidate PPREs are illustrated within

the 1-kb region of the human LPCAT3 promoter. PPRE1 is conserved in mouse, rat, bovine and human LPCAT3 promoters. (*B*) The proximal PPRE1 is sufficient for PPARα response. A series of promoter-reporter deletion constructs were made. Huh7 cells were co-transfected with PPAR-reporter vector or negative control (pGL3) vector along with PPARα expression vector. After 16 hr, transfection medium was changed to growth medium. After 24 hr of transfection, cells were treated with PPARα agonist (WY14643, 20 μM). After 18 hr treatment, luciferase assays were performed, and relative reporter activity (percentage) was determined. Values are mean ± SD, n = 3. (*C*) PPARα binds to PPRE1. Electrophoretic mobility shift assays were performed with ^{32}P-labeled fragments of the LPCAT3 promoter extending from nt −133 to −97 in the presence of PPARα, RXRα, or both. Arrow indicates the position of the PPARα/RXRα complex. WT and mutant (mut) oligonucleotide competitors were included at a 5-fold or 25-fold molar excess. Sequences of the WT and mutant oligonucleotides are shown with putative nuclear receptor half-site sequences capitalized. A representative blot from three independent experiments is shown. (*D*) Chromatin immunoprecipitation (ChiP) assay on liver of WT mice. C57BL/6 mice were injected with fenofribrate (300 mg/kg/day) for 10 days. The ChiP analysis was carried out using IgG or anti-PPARα antibody. The procedure was as described in Experimental Procedures. A representative blot from three independent experiments is shown.

Supplemental Figure 9. Effect of LPCAT3 deficiency on apoptosis, ER stress, and proliferation. (*A*) Real-time PCR for ER stress markers: Ire1α, Bip, and Perk. (*B*) Real-

time PCR for cell proliferation marker: Ki-67. (*C*) Small intestine caspase 3 immunostaining. (*D*) Quantification of caspase 3 levels. Values are mean ± SD, n = 4.

Supplemental Table 1. mRNA measurement by real-time PCR

	WT	LPCAT3 KO
Small intestine		
CD36	100±35	130±60
NPC1L1	100±50	120±25
ABCG5	100±40	110±35
ABCG8	100±30	100±40
MTP	100±20	530±80*
ABCA1	100±50	90±25
Liver		
ABCA1	100±25	120±40
ABCG1	100±40	110±25
SRB1	100±40	110±35
MTP	100±30	380±60*

Value, mean ± SD, n = 5, *P < 0.01.

Supplemental Table 2. Measurement of LysoPC subspecies by LC/MS/MS

	16:0	16:1	18:0	18:1	18:2	20:1	20:2	20:4	22:6	Total
Hepatocytes(ng/mg protein)										
WT	214±10	21±2	85±11	119±19	267±32	11±1	12±2	39±8	51±8	819±99
LPCAT3 KO	213±29	24±6	80±16	135±39	186±30*	10±2	11±1	22±3*	77±12*	758±81
Enterocyte(ng/mg protein)										
WT	560±66	13±2	338±81	110±30	213±42	26±5	15±3	25±3	58±16	1358±192
LPCAT3 KO	502±89	18±4	390±52	159±24	190±31	30±7	12±2	33±5	69±24	1403±236

Value, mean ± SD; n = 5; *P < 0.05.

Supplemental Fig. 1. Li et al.

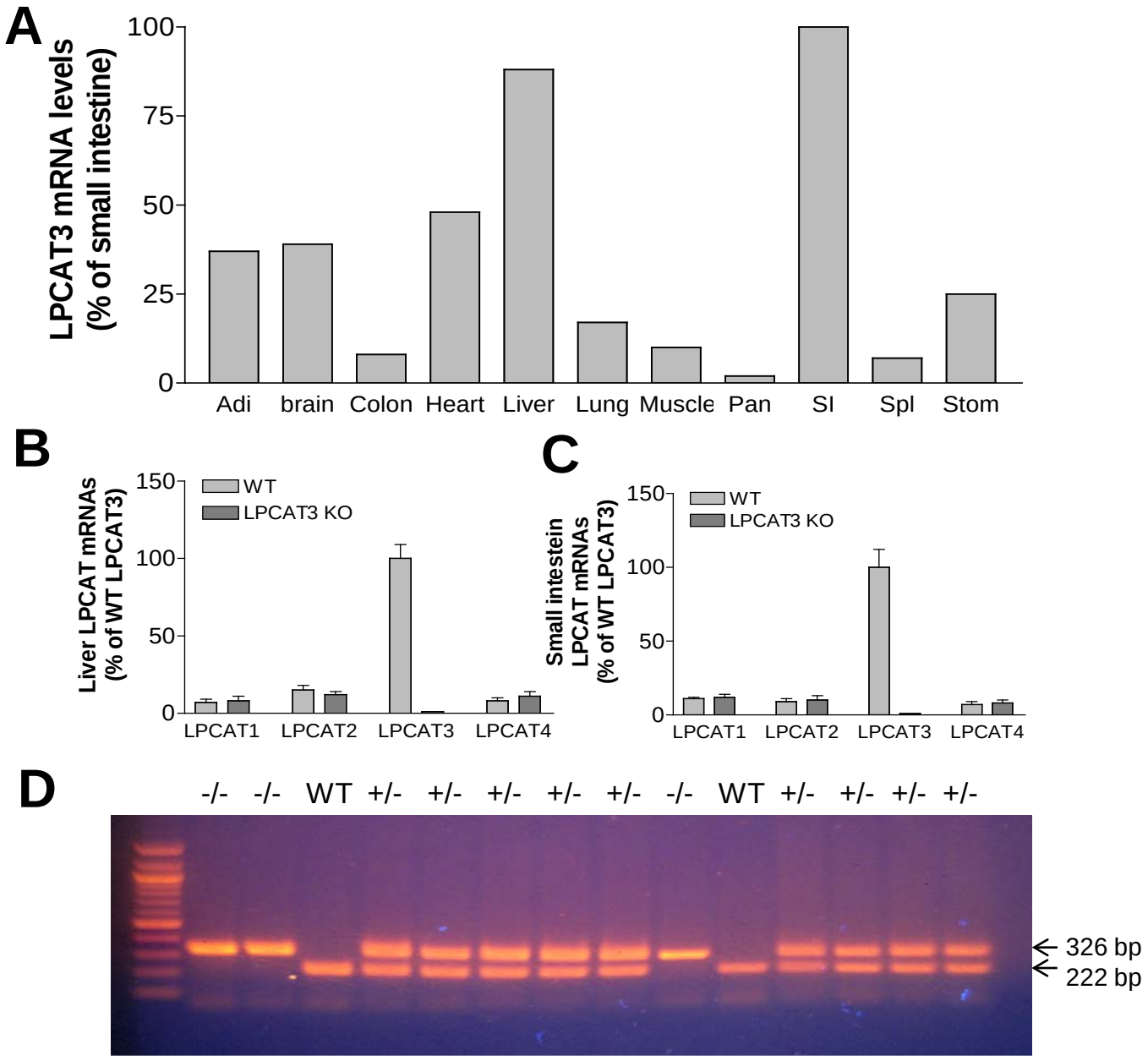

Supplemental Fig. 2. Li et al.

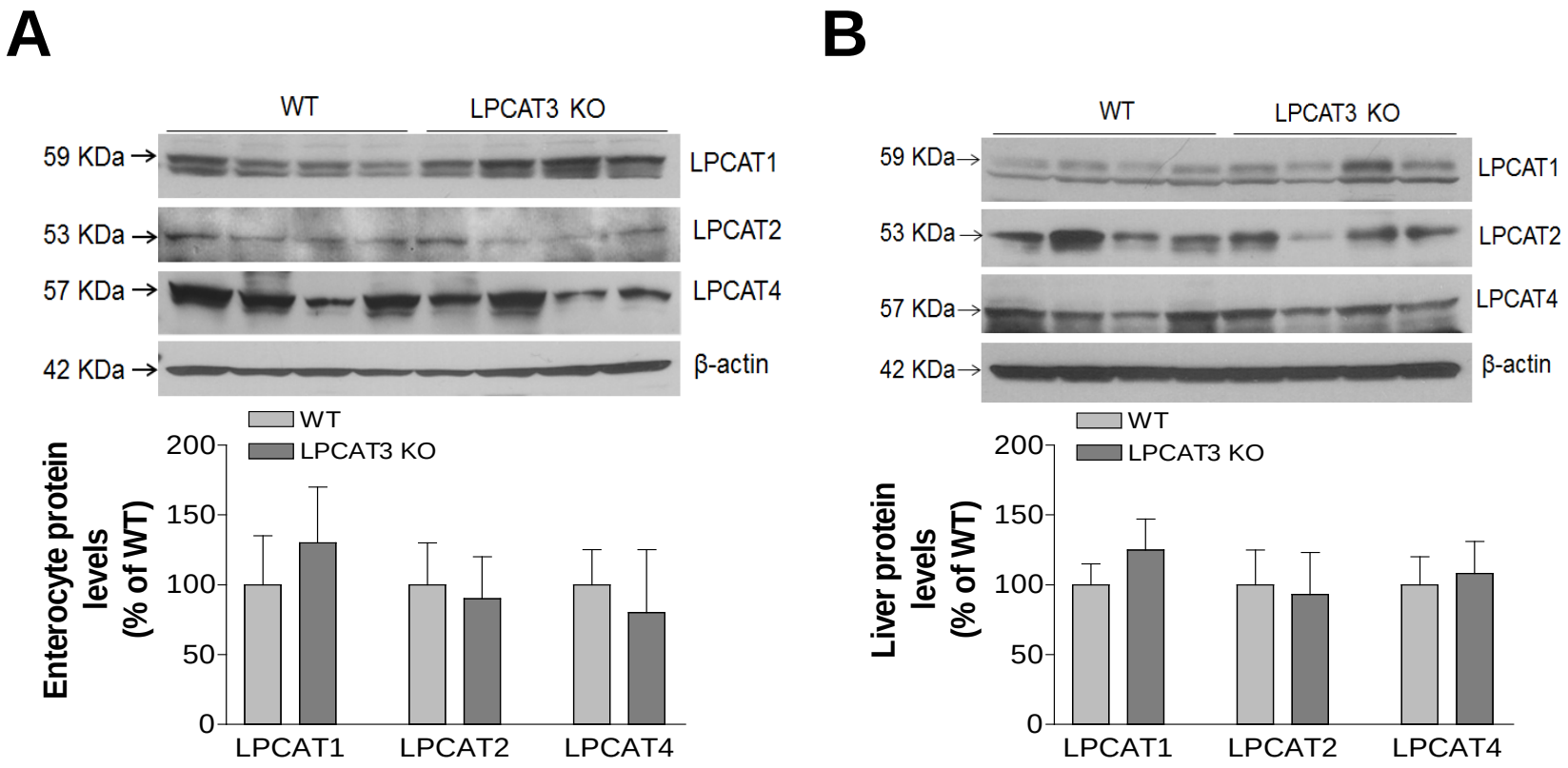

Supplemental Fig. 3. Li et al.

Supplemental Fig. 4. Li et al.

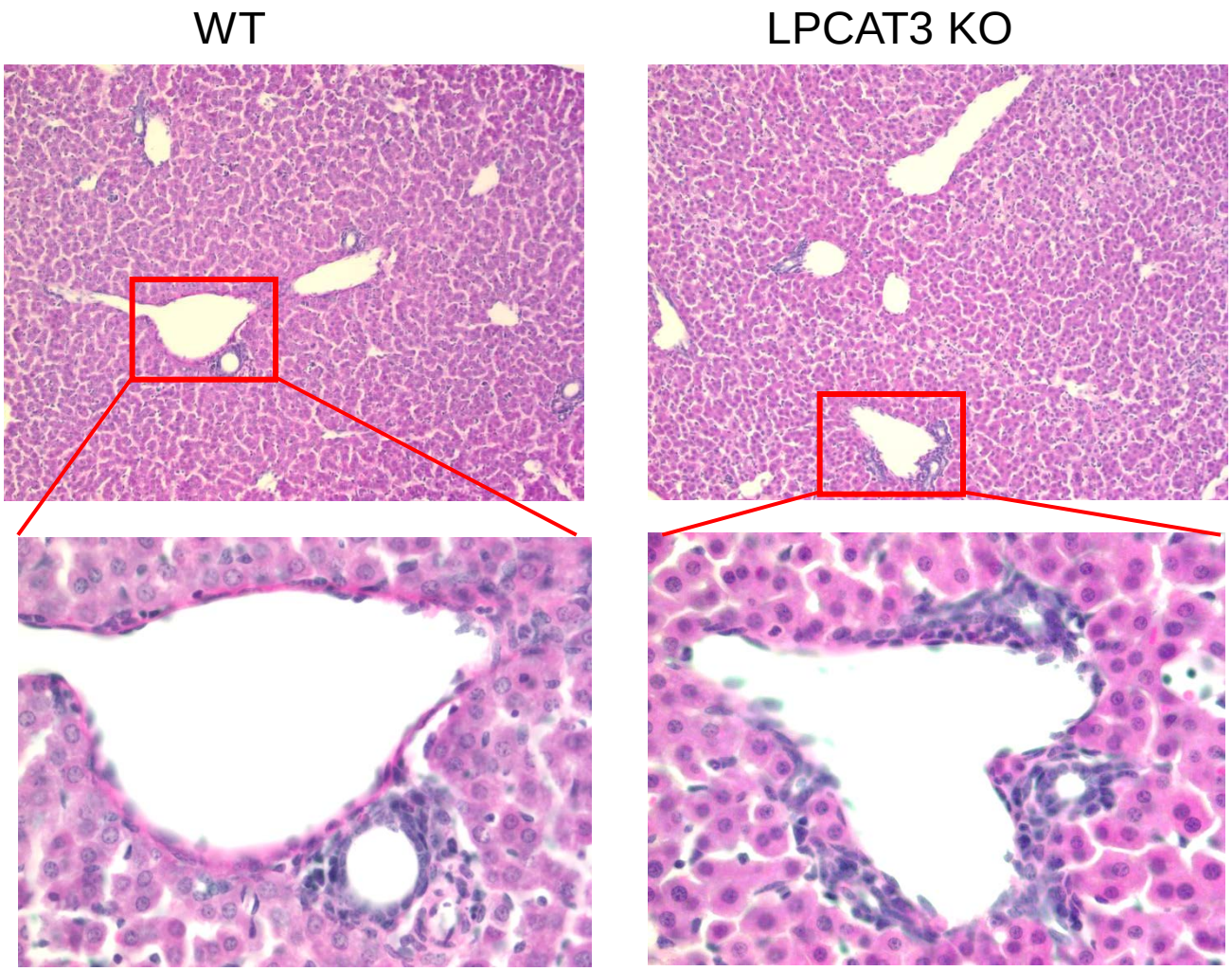

Supplemental Fig. 5. Li et al.

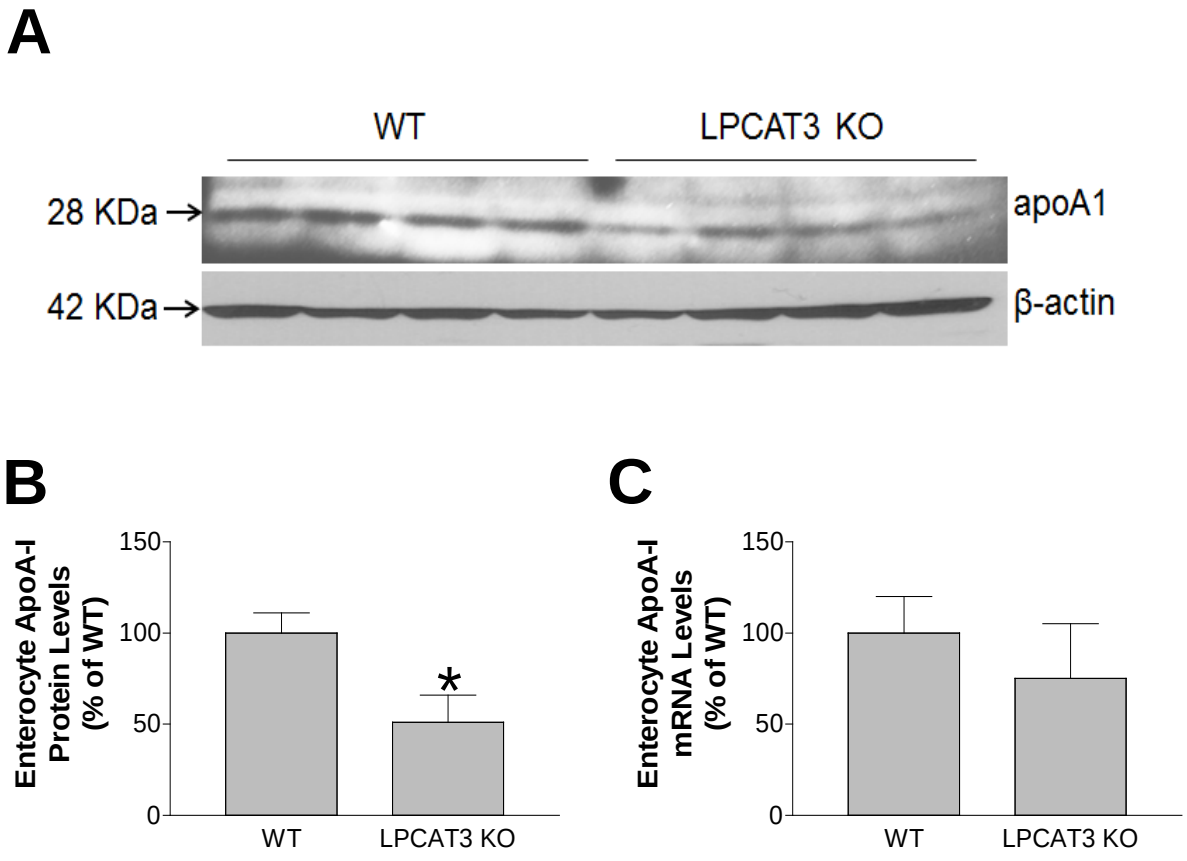

Supplemental Fig. 6. Li et al.

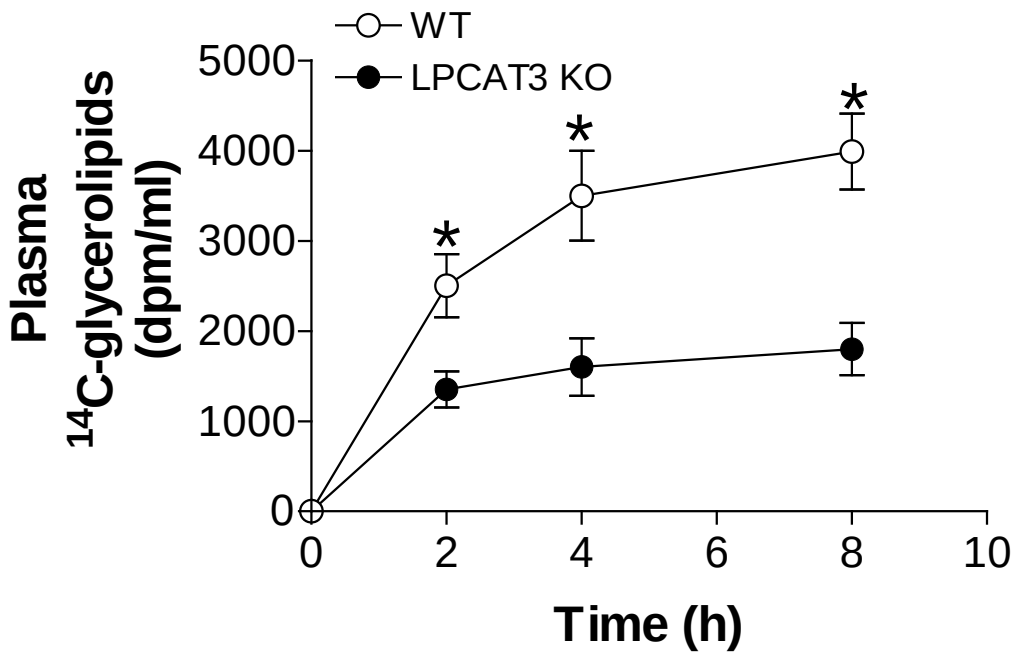

Supplemental Fig. 7. Li et al.

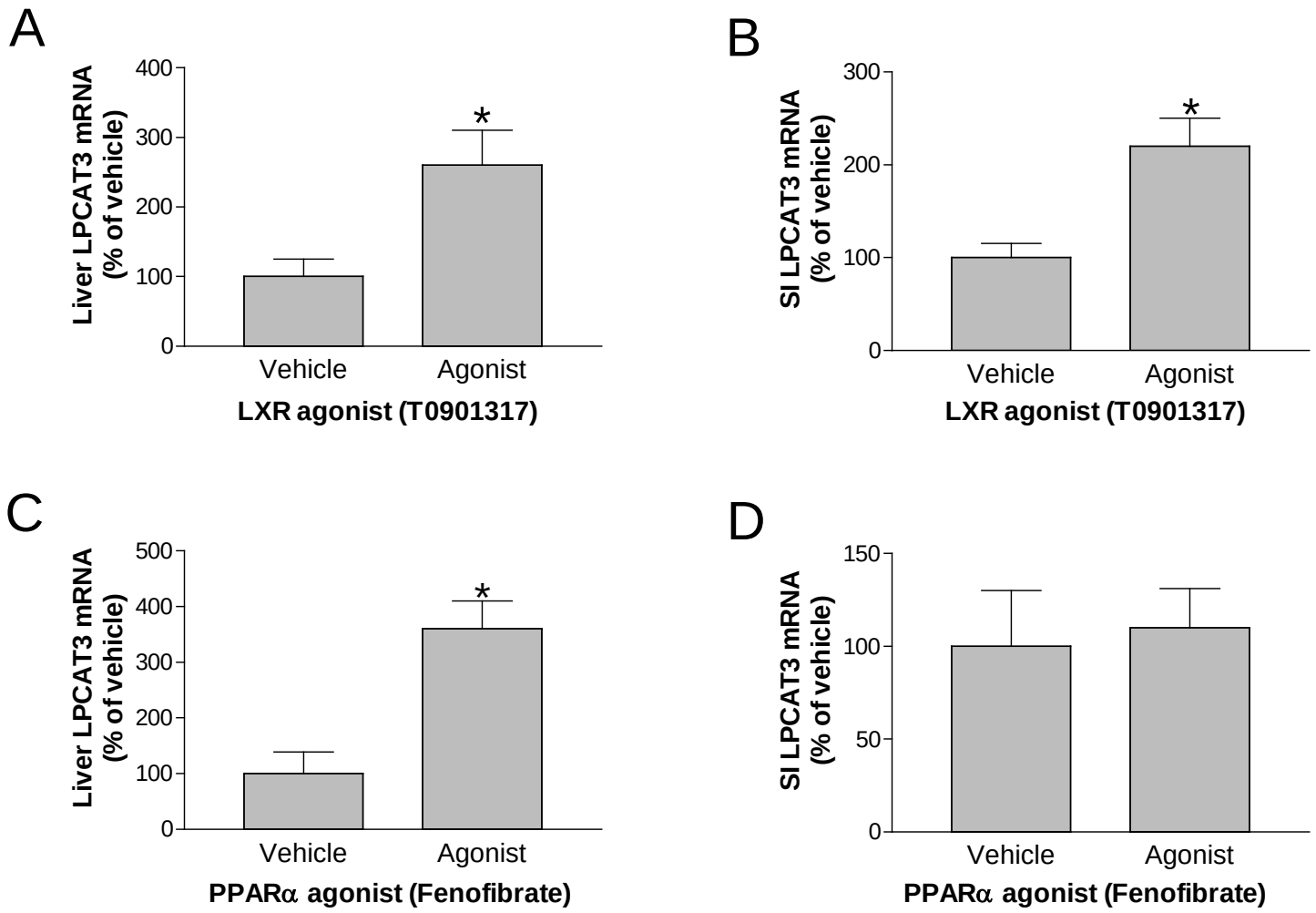

Supplemental Fig. 8. Li et al.

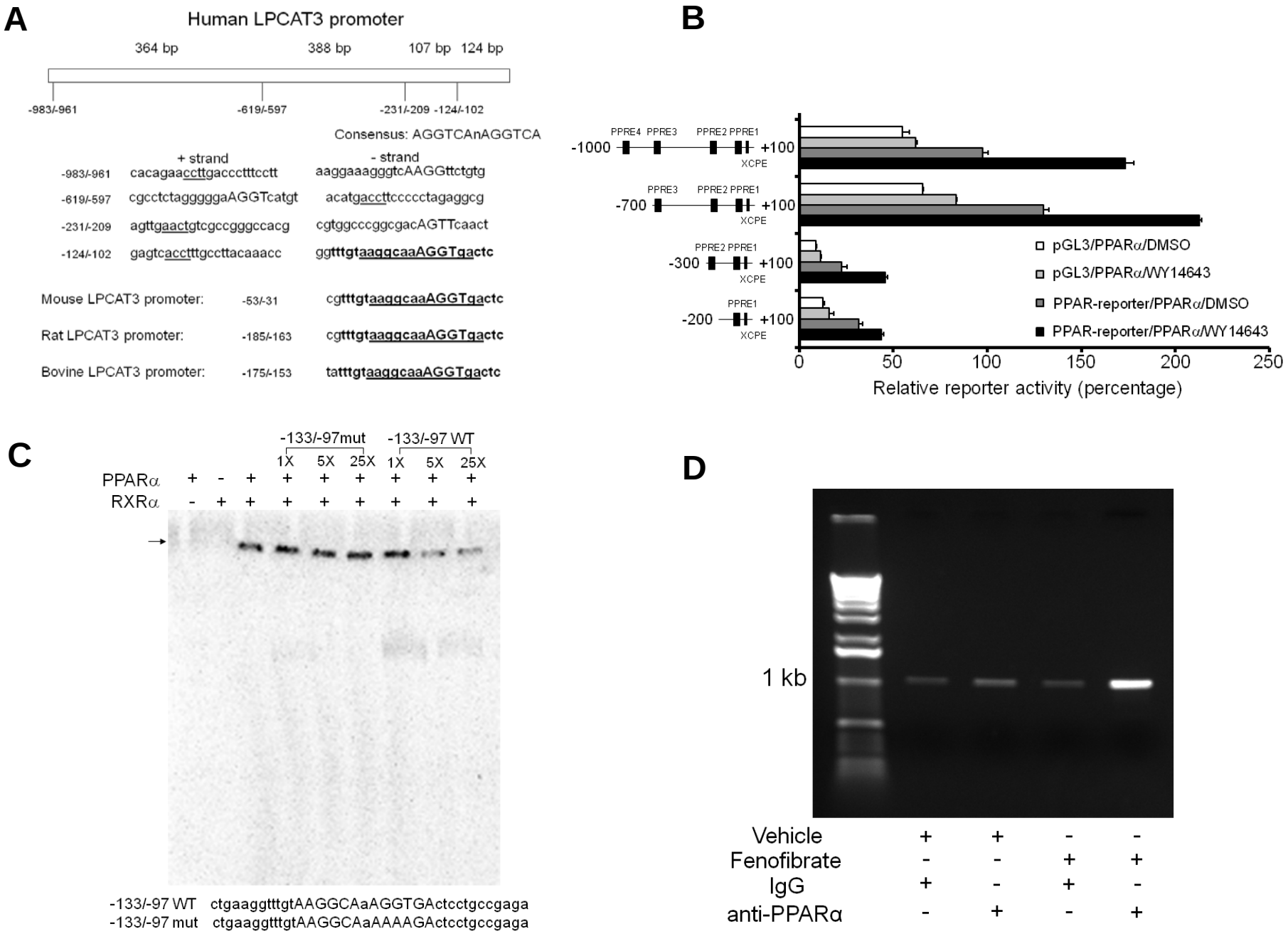

Supplemental Fig. 9. Li et al.